Afyon Kocatepe Üniversitesi Fen ve Mühendislik Bilimleri Dergisi

Afyon Kocatepe University Journal of Science and Engineering

AKÜ FEMÜBİD **18** (2018) **011203** (807-819) AKU J. Sci. Eng. **18** (2018) **011203** (807-819)

DOİ: 10.5578/fmbd.67761

Araştırma Makalesi / Research Article

Investigation of Corrosion Behaviours Hydroxyapatite (HAP) coated Ti6Al4V Implants by Using Electrochemical Deposition Method

Aysel Büyüksağiş[1], Yusuf Kayalı[2]

[1] *Afyon Kocatepe University, Faculty of Arts and Sciences, Department of Chemistry, Afyonkarahisar, TURKEY*

[2] *Afyon Kocatepe University, Faculty of Technology, Department of Metallurgical and Materials Engineering, Afyonkarahisar, TURKEY*

e-posta: absagis@aku.edu.tr

Geliş Tarihi:03.01.2018 ; Kabul Tarihi:04.12.2018

Keywords
Electrophoresis; Hydroxyapatite; Corrosion; Ti6Al4V.

Abstract

In this research, hydroxyapatite (HAP) has been coated on the Ti6A14V alloy surface by electrophoresis method. In this electrophoresis method, $NH_4H_2PO_4$ is taken as P precursor and Ca $(NO_3)_2.4H_2O$ is taken as Ca precursor to obtain HAP coating. Additionally, 5 N NaOH pre-treatment surface operation (PTSO) has been applied to Ti6A14V. PTSO are effective on clinging of HAP coating to the surface. The corrosion behaviours of uncoated and HAP coated samples are examined in simulated body fluid (SBF) after for holded 7, 14, 21 and 35 days in SBF. HAP coatings have obtained by electrophoresis method was not showed inhibition for preventing corrosion. The surface images of the samples were described by scanning electron microscope (SEM), energy dispersive X-ray analysis (EDX), and X-ray diffraction (XRD). From SEM images have been observed open pores and connections among pores in the coating, which increases osteointegration. It is noted in EDX analyses of the surfaces of the HAP coated samples that there is Ca, O and P on the surface. It is seen in XRD analysis of HAP coated samples that there are TiO_2, HAP and calcium phosphate structures on the surfaces.

Elektrokimyasal Biriktirme Yöntemi ile Hidroksiapatit (HAP) Kaplanmış Ti6Al4V İmplantlarının Korozyon Davranışlarının İncelenmesi

Anahtar kelimeler
Elektroforez; Hidroksiapatit; Korozyon;Ti6Al4V

Özet

Bu araştırmada, hidroksiapatit (HAP) elektroforez yöntemi ile Ti6A14V alaşımı yüzeyine kaplanmıştır. Elektroforez yönteminde HAP kaplama elde etmek için, $NH_4H_2PO_4$, P öncüsü olarak ve $Ca(NO_3)_2.4H_2O$, Ca öncüsü olarak alınmıştır. Ek olarak, Ti6A14V'ye 5 N NaOH ön-muamele yüzey işlemi (PTSO) uygulanmıştır. PTSO, HAP kaplamanın yüzeye yapışmasında etkilidir. Kaplanmamış ve HAP kaplanmış numunelerin korozyon davranışları simüle vücut sıvısında (SBF) 7, 14, 21 ve 35 gün bekletildikten sonra incelenmiştir. Elektroforez yöntemiyle elde edilen HAP kaplamalar korozyonun önlenmesi için inhibisyon göstermemiştir. Numunelerin yüzey görüntüleri taramalı elektron mikroskobu (SEM), enerji saçınımlı X ışınları (EDX) ve X ışınları difraksiyonu (XRD) yöntemleri ile tanımlanmıştır. SEM görüntülerinden, açık gözenekler ve kaplamada gözenekler arasındaki bağlantılar gözlenmiştir ve bu da osteointegrasyonu arttırmaktadır. HAP kaplamalı numunelerin yüzeylerinin EDX analizlerinde yüzeyde Ca, O ve P olduğu not edilmiştir. HAP kaplamalı numunelerin XRD analizinde yüzeylerde TiO_2, HAP ve kalsiyum fosfat yapılarının olduğu görülmektedir.

1. Introduction

Titanium alloys are biomaterials frequently used as orthopaedic inserts due to their excellent durability and excellent hardness (compared with other biomaterials). Nevertheless, Ti alloys are sensitive to corrosion ions contained by body fluids. Especially, metallic ions react with the ions in body fluid, and then this affect to the neighboring textures. To prevent this adverse effects, biomaterials are coating hydroxyapatite [Ca_{10} $(PO_4)_6(OH)_2$-HAP] (Kwok *et al.* 2009, Rath *et al.* 2012, Benea *et al.* 2014a, Benea *et al.* 2015). HAP is widely known as a coating material, near identity of bone chemical composition and its talent to chemical bond conjuction bone smoothly for dental health and orthopedic implants a great of years. Many HAP coating techniques were applied to metals; for instance air plasma spraying, sol-gel deposition, perfusion electrodeposition, plasma electrolytic oxidation, hot pressing, laser coating, sputter coating, biomimetic coating, and electrophoresis (EPD). Between several coating methods, EPD offers a lot benefit like, the capability to control electrochemical characteristic property, the capability to check out the thick and morphology of the deposited layer, the ability to leave relatively uniform coatings on complicated forms, a higher sediment rate checks most coating processes and needs is lower priced at purchase the instruments.

Generally, HAP covering on Ti alloys is poor bonded to metal. Some surface qualification methods are proposed to increase surface roughness and interactions of coating material as mechanically and chemical methods; these are blasting, grit blasting, acid treatment, alkali treatment, hydrogen peroxide treatment, hydrothermal-electrochemical methods. These techniques develop adhesive ability only slightly. Pre-treating the Ti6Al4V substrate with NaOH, shows that is increasing adhesion and crystallinity, a three-dimensional porous network of sodium titanate gel was observed on the Ti6Al4V surface by after NaOH pretreatment. The goal of alkali treatment is create a sodium titanate layer which can induces apatite formation by providing surface functional sites composed of Ti-OH groups, which are effective for apatite nucleation.

Benea *et al.* (2014b) reported; first of all anodic polarization applied on Ti6Al4V alloy using DC power (at 100 voltages for 2 min.). Later samples soaked 5 M NaOH solution at 60 ^oC for 10 min. Electrodeposition of calcium phosphate was applied at room temperature and applied by a constant current density of 0.6 $mAcm^{-2}$ about 45 min.

Electrochemical analysis tested in Fusayama-Mayer saliva solution. The conclusions showed coating increased corrosion resistance of Ti6Al4V alloy. Du *et al.* (2014) in their study Ti6Al4V substrates were applied pre-treatment surface operation with 8 M NaOH different times at 60 ^oC. HAP coated on Ti6Al4V by hydrothermal-electrochemical method containing NaCl, $K_2HPO_4{\cdot}3H_2O$, and $CaCl_2$ solution at 120 °C and achieved by a steady current density of 1.25 mA/cm^2 about 120 min. Experimental results showed after 48 h NaOH treatment magnitude of pore in HAP network increased quite. Drevet *et al.* (2010) in their research calcium phosphate coating were applied on Ti6Al4V alloys using pulsed electrodeposition method with use different hydrogen peroxide (H_2O_2) volumes at 60 ^oC. HNO_3 and HF acid mixture applied to substrates. The outcames of experimental results showed calcium phosphate coating a good adhesion and homogenity rather than classical electrodeposition. HAP and β-TCP formed on the Ti6Al4V alloy surface.

Our research is with the following features different from literature studies. The aim of this paper is to investigate the effect of NaOH PTSO on the corrosion and morphologies of hydroxyapatite (HAP) coated and uncoated Ti6Al4V alloy. Additionaly, to compare the electrochemical behavior of the HAP coated and uncoated Ti6Al4V surface with NaOH PTSO by using open-circuit potential measurement (OCP), potentiodynamic polarization and electrochemical impedance spectroscopy (EIS) methods in SBF. In this study, 5 N NaOH PTSO was applied on Ti6Al4V alloys at 24 h

60 °C. Before HAP coating, 45 minutes of nitrogen gas was passed through the electrophoresis solutions. Between the anode and cathode distance has been adjusted as 0.5 cm. HAP Coatings was done for 1 hour under 4.5 V voltage at 85 °C with pH=5.5. HAP coated Ti6Al4V substrates sintered in muffled furnace. Then HAP coated and uncoated electrodes waited in simulated body fluid (SBF) at different time and later electrochemical tests made in SBF. SEM microphotographs took by LEO 1430 VP.

The same time EDX analyzes (Röntec EDX device and the Quantax soft program connected to the SEM microscope) were also performed on these samples. The structural properties of the HAP coating on Ti6Al4V were analyzed using the Shimadzu brand XRD-6000 model.

2. Materials and Methods

2.1 HAP coating by electrodeposition method of substrates and pre-treatment surface operation

Commercially available Ti6Al4V (Grade 23) cylinder bar, with dimensions of Ø15 mm×10 mm, were mechanically polished with P200, P400, and P800, P1000, P1200 abrasive papers. Subsequently, samples were ultrasonically cleaned for 15 minutes in acetone, ethanol, and then bidistilled water. Subsequently they were dried in an oven at 40 °C. All sides of the Ti6Al4V was then sinked with epoxy resin except the single surface (surface area is 2.0096 cm^2). All chemicals were used Merck reagants. The coating electrolyte was prepared a mixture of 0.042 M Ca $(NO_3)_2.4H_2O$, 0.025 M (NH_4) H_2PO_4, 0.15 M $NaNO_3$ and 10 mlL^{-1} H_2O_2.

Temperature of the electrophoretic solution was set up 85 °C, the pH was adjust 5.5 by using tris (hydroxymethyl) aminomethane (TRIS) and HCl solutions. For pH measurements used Hanna model pH meter. Electrophoretic solution and SBF were stored in the fridge at 4 °C after preparation and pH adjustment. The electrophoretic solutions were de-aerated with N_2 for 45 min prior to the coating process. The platinum anode electrode was placed as parallel to the surface of the Ti6Al4V cathode electrode (the distance between the electrodes was adjusted as 5 mm). Electrophoretic deposition tests were carried out at voltages 4.5 V using a D.C. voltage regulator at one hour. At the end calcium phosphate coverings on Ti6Al4V alloy surface were get through electrochemical deposition. Deposition working temperature conditions were supported by using thermostat circulating water bath. The HAP coated samples after deposition were cleaned with double distilled water, and dried oven at 40 °C.

Sintering process; firstly HAP coated samples have been put into muffled furnace and then the temperature of furnace was set up to 400 °C. When the temperature is reached 400 °C, test samples were kept for 10 minutes this temperature. When the furnace temperature was increased every 100 °C and samples were kept 10 minutes these temperatures, finally test samples were kept for 30 minutes at 850 °C, and furnace turn off. The substrates were taken from the muffled furnace one day later.

2.2 Electrochemical measurements and surface morphology studies

The work plan of experimental study is given below:

a) NaOH PTSO was applied to bare electrodes. After surface treatment, the electrodes were dried at 40 °C for 1 hour.
b) SBF is similar to body fluid structure. The pH of the SBF was adjusted 7.4 with 0.1 M TRIS and 0.1 M HCl solutions. $NaNO_3$ was added to inhibit bacterial production in SBF.
c) Electrodes are immersed in SBF, the chemical composition of SBF is as follows: Na^+ (142 mM), K^+ (5.0 mM), Ca^{2+} (2.5 mM), Mg^{2+} (1.5 mM), Cl^- (147.8 mM), HCO_3^- (4.2 mM), HPO_4^{2-} (1 mM), SO_4^{2-} (0.5 mM).
d) 3 test electrodes were placed in each brown glass bottle. Since the surface area of the Ti alloy is 2.0096 cm^2, 25 mL of SBF solution per sample was added and totaly of 75 mL SBF was added. Glass bottles were placed in shaking water bath as the shaking speed was adjusted 80 rpm and the bath temperature was set up as to 37 °C.

e) Uncoated and HAP coated Ti6Al4V alloys were waited in bottles with incubation times of 7, 14, 21, 35 days for 37 °C and pH = 7.4, respectively in the SBF solution. The SBF solution has been changed every two days to adjust pH 7.4 and solution temperature 37 °C. Adjusted SBF was added to the bottles.
f) After waiting, the samples were washed with bidistille water and the sample was dried at 40 °C for 3 hours.
g) Corrosion tests of the samples were then investigated in SBF at 37 °C.

The corrosion properties of Ti6Al4V alloys after exposure in SBF for diverse time at 37 °C were studied by electrochemical techniques. All electrochemical tests were carried out using a Gamry Reference 600/ZRA potentiostat/galvanostat (USA) and Echem analyst soft programme. The electrochemical experiments open circuit potential (OCP), potentiodynamic polarization and electrochemical impedance spectroscopy (EIS) were performed to naked and HAP coated Ti6Al4V samples in SBF. All potentials were measured with respect to a saturated calomel electrode (SCE, 0.244 V versus SHE at 25 °C) as the reference electrode. To avoid the potential drop between the saturated calomel electrode (SCE) and the working electrode, the SCE was brought close to the working electrode with the help of a Lugin-Haber capillary. After the incubation times in the SBF, the uncoated and HAP coated electrodes were immersed in the SBF solution and allowed to stand for about 30 minutes, after which current-potential curves were obtained. Current-potential curves were obtained at a scanning speed of 1 mV/s by the potentiodynamic method. Linear polarization and EIS measurements were made. The electrochemical experiments were performed in a conventional three-electrode cell consisting of: Ti6Al4V alloy substrates were used as the working electrode while platinum was used as the counter electrode, and saturated calomel electrode (SCE) as the reference electrode. In order to test the repeatability of the results, the experiments were performed in triplicate. Using the potentiodynamic method, the current potential curves of the in the SBF medium were obtained.

Corrosion characteristics determined in this study are corrosion rate (i_{cor}), corrosion potential (E_{cor}), anodic and cathodic Tafel slopes (β_a and β_c). After electrochemical measurements, surface images are taken from by LEO 1430 VP SEM microscope. EDS spectrums are also taken over same samples. XRD has been used to determine structure of HAP on substrates.

3. Results and Discussions

3.1 Electrochemical results and discussions

The electrophoretic solutions were de-aerated with N_2 for 45 min. prior to the coating process. The aim of this is to decrease the quantity of distribute CO_2 gas and thus stop the constitution of $CaCO_3$ sediments (Blackwood and Seah 2009). $NaNO_3$ was added to support the ionic forces of the electrolytes, and H_2O_2 was added to wipe off the rise of H_2 gas and then advance the accumulation of thick. Actually electrodeposition (EPD) contains a two-step processing; primary stage, charged ions hanging in a fluid may be move to an electrode under the effect of an electric field (electrophoresis). Secondly stage, the particles can be deposit on the electrode forming a relatively dense and uniform compact or film (Song *et al.* 2008). Water-based suspensions supports gas formation from the hydrolysis of water, from blocking up the residue of homogenous cohesive film and small holes (Abdeltawab *et al.* 2011, Stoch *et al.* 2001, Radice *et al.* 2010). HAP coating of the surface rely on two circumstances: (i) mechanical interlocking, can be increase by surface pre-treatment operations (Rigo *et al.* 2004, Jonasova *et al.* 2004), and (ii) chemical bonding is increased by thermal processing (Kwok *et al.* 2009).

After 7, 14, 21 and 35 days waited in SBF, The Tafel and Nyquist curves obtained for the uncoated and HAP coated Ti6Al4V alloys are given in Figures 1, 2, 3 and 4.

The electrophoresis solution stirr rate has two effects. The firstly is the useful effect of the centrifugal forces moving away the hydrogen bubbles from the surface gives more yield calcium phosphate sediment allowing a more cohesive layer to form. Secondly and perhaps more main effect of turning increases the rates of migration of both the reactants to, and the products from, the Ti6Al4V surface. Therefore the best mixture speed is a compromise between these two effects (Blackwood and Seah 2009, Drevet *et al.* 2010).

On the other hand, when H_2O_2 add to the electrolyte, hydrogen gas evolution visually decrease on Ti substrate surface during the electrophoresis, some calcium phosphates similar cauliflower structures were seen in the electrolyte. The Na_2TiO_3 layer has been supported HAP formation to interchange ions with Ca^{2+} in electrolyte, so that it converted to $CaTiO_3$. The $CaTiO_3$ structures helps for the formation of HAP, it behaves as a binding layer between the HAP and the Ti6Al4V substrate.

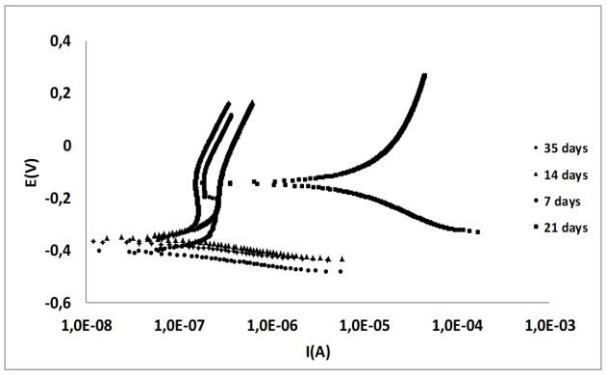

Figure 1. Tafel plots of uncoated Ti6Al4V alloys in SBF.

In addition, when H_2O_2 reagent adds to the electrodeposition solution were lost the craters and holes and the pins are collected on the substrate (Fig.5). When a Ti6Al4V substrate is treated with NaOH, a three dimensional porous hydrogel layer made of sodium titanate is formed on the Ti6Al4V surface. In addition, Wang *et al.* (2009) have been reported that directly immersing Ti alloys in NaOH supported HAP nucleation, advancing the maturation of Na_2TiO_3 layer.

The gel can be transformed to Ti-OH groups during hydrothermal-electrochemical deposition, which will contribute to the formation of hydroxyapatite.

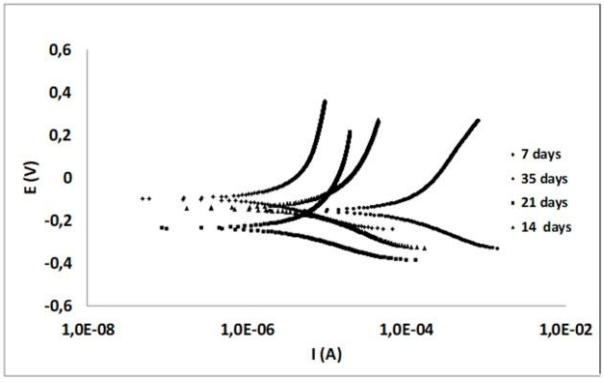

Figure 2. Tafel plots of HAP coated Ti6Al4V alloys in SBF.

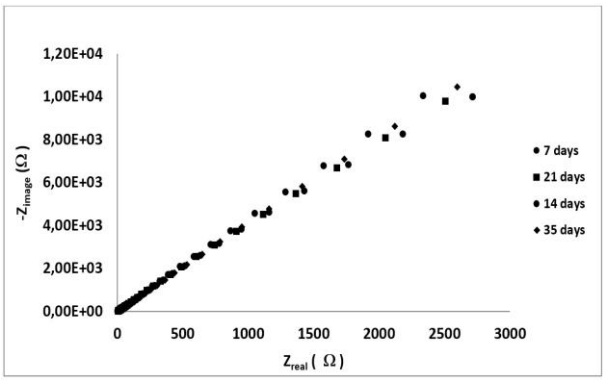

Figure 3. EIS plots of uncoated Ti6Al4V alloys in SBF.

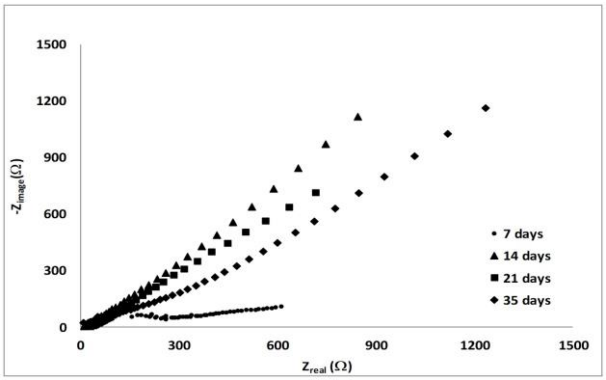

Figure 4. EIS plots of HAP coated Ti6Al4V alloys in SBF.

Besides this, the gel's porous constitution can produce more nucleation sites, thus build on the adhesion strength among the Ti6Al4V electrode and the deposited HAP layer (Wang *et al.* 2009, Ban and Hasegawa 2002, Rakngarm and Mutoh 2009). Moreover, because of the fact that the restricted three-dimensional network structure, for the HAP layer manufactures a choosing field.

Corrosion characteristics calculated from current potential curves obtained from electrochemical experiments are given in Table 1.

As the pretreatment time rises, the sodium titanate gel layer set off more thick, allowing for the production of more Ti-OH groups for the time of hydrothermal electrochemical deposition. The greater amounts of Ti-OH groups will allowe further nucleation stuations, thus promoting the formation of the second layer, which produces dandelion-like hydroxyapatite. The dandelion-like shape of this second layer might arise because of less space limitation (Benea *et al.* 2014a, Benea *et al.* 2014b, Du *et al.* 2014, Bir *et al.* 2012). When Table 1 is examined, the lowest corrosion rate was seen in the Ti6Al4V alloy, which has remained in SBF for 35 days. This shows that the Ti6Al4V alloy is exposed to corrosion for during first 7 days, then Ti6Al4V surface were covered with the oxide and hydroxides, there by reducing the corrosion over time. At 7, 14 and 35 day waiting times, the anodic Tafel slope (β_a) is as large as 1×10^{15}. This shows that the reaction on the surface of Ti6Al4V is controlled by anodic diffusion control.

The samples immersed of 14 days in SBF, the anodic Tafel slope is smaller than 1.099 others. When the cathodic Tafel slope (- β_c) is examined, it is observed that the β_c increases as the corrosion rate decreases. The same phenomenon is seen in the corrosion rate values. Rp values have also been supported this.

Table 1. Corrosion characteristics of uncoated and HAP coated Ti6Al4V alloy deposited at different times in SBF.

	Immersed Days	βa (V/decade)	- βc (V/decade)	i_{corr} (μA/cm²)	E_{corr} (mV)	Corrosion Rate (mpy)	R_p (kΩ)
uncoated	7 days	$1x10^{15}$	$59,4x10^{-3}$	0,103	-424	$36,04x10^{-3}$	95,91
	14 days	1,099	$65,70 x10^{-3}$	0,094	-355	$32,77x10^{-3}$	98,32
	21 days	$1x10^{15}$	$75,20x10^{-3}$	0,116	-406	$40,37x10^{-3}$	111,00
	35 days	$1x10^{15}$	$45,00x10^{-3}$	0,079	-372	$27,5x10^{-3}$	85,11
HAP coated	7 days	$852x10^{-3}$	$116x10^{-3}$	50,00	-85,50	17,44	0,450
	14 days	$503x10^{-3}$	$179x10^{-3}$	2,36	-149,00	$824x10^{-3}$	10,64
	21 days	$478x10^{-3}$	$166x10^{-3}$	2,13	-305,00	$742x10^{-3}$	11,36
	35 days	$643x10^{-3}$	$170x10^{-3}$	1,40	-77,50	$488x10^{-3}$	21,62

When looked at Table 1, HAP coated part is examined, the corrosion rate in HAP coated samples is considerably higher than the uncoated surfaces. Ti6Al4V shows a two-layer passive film containing of an inner barrier and an outer porous layer to display good osseointegration. The migration of these bone cells to the passive filmin pores in the body fluid, and the stronger of the adhesion between the Ti6Al4V and bone. This stuation assist to protect the metallic material from corrosion in the dense inner barriers layer (Karthega *et al.* 2007). When the HAP coating has pores, a conductive path is formed between the metallic conductor and the electrolyte. The HAP coating acts as a semiconductor blockade to stop interaction of the substrate with the solution. Water and chloride ions enter the coating and corrosion is begun.

It is seen that, Table 1, HAP coated section; the corrosion rate decreases as the waiting time increases. The corrosion rate of the hydroxyapatite coated Ti6Al4V alloy is increased compared to the corrosion behavior of the uncoated specimens. The following factors have been effective in increasing the corrosion rate;

1) In the electrochemical coating, 4.5 V voltages have been applied to the electrode coated with DC power supply.
2) The muffle furnace was used after electrochemical coating; sintering process was made at high temperatures (400-850 ° C).
3) With an inert atmosphere (such as argon in N_2) hasn't been supported for the muffle furnace during sintering. Because there was no such system in the furnace. For this reason, HAP coated specimens have been subjected to high temperature corrosion.

In Table 1, HAP coated section; as the waiting time increased, the corrosion rate values decreased and the Rp values increased. These results are consistent with the corrosion rate values.

The negatively charged ions have merged with Na^+ ions in electrophoresis solution, for the

manufacture of a sodium titanate hydrogel layer (Balamurugan *et al.* 2009). In the study carried out by Oh and Jin (2006) have shown that the formation of hydroxyapatite on TiO_2 nanotube surface containing sodium titanate is remerkably speed up.

When the pH of the electrolyte changes (such as pH 6.0) the acid phosphate groups are successfully transformed to PO_4^{3-} and stoichiometric HAP can be directly deposited on the cathodes.

Schmidt et al. (1998) described, deterioration and pitting corrosion ascribe to the due to decreased oxygen amount at the interfilm between the passive film and the implanted film. The implanted ions act as a barrier to the diffusion of oxygen. The changes of the corrosion resistance of the HAP coated Ti6Al4V alloy after long-time immersed in SBF can be connected with the changes of the chemical integration of the surface layer and its rebuilding. After sintering, the HAP coating take place more uniform owing to the bunching with each other of the pieces. The HAP coating acts a barrier between the substrate and the electrolyte; it is prevent migration of ions and electrons, thus decreasing the electrochemical reaction rate. The HAP coatings and TiO_2 act like semiinsulator, and then they show better corrosion resistance. Corrosion forms between the substrate surface and HAP coating, the corrosive ions passes the HAP coating by diffusion, electrochemical corrosion reactions form on the interface. Zhang *et al.* (2005) recorded that the corrosion process of HAP coating with pores involved two steps. Firstly, hydrogen ions (H^+) are produced at the interface area where corrosion occurs:

$$Ti + 2\ H_2O \leftrightarrow TiO_2 + 4H^+ + 4é \quad (1)$$

It is then followed by the dissolution of HAP in the high H^+ concentration area:

$$Ca_{10}(PO_4)_6(OH)_2+2H^+\leftrightarrow 10Ca^{2+}+6PO_3^{2-}+H_2O \quad (2)$$

The local pH of the interface is very low in view of the fact that the H^+ can not be well cycled out of the interlayer and resolution of HAP catalytically accelerated. When the corrosion begins, it cannot stop till the whole interfacial HAP is dissolved. The coating then breaks down at the coating and substrate interfacial field. The distinction in corrosion resistance of different HAP coatings, which have diversified degrees of porousness, is stable with this corrosion mechanism.

According to Kumar *et al.* (1999), to form H_2 molecule, hydrogen atom react with each other. The result of this, HAP coating can not accumulate on surface formed with hydrogen balloons. Because this phase doesn't mass transfer mechanism happen consequently of HAP coating doesn't form. H_2 gase behave as an insulator. For ion migration and diffusion must be passed through the bubble-HAP interface. The growth of HAP around the bubbles results in a capture. When this spherical gas bubbles have been burst, HAP crystals will continue to form. In Table 1, the contribution of the 5 N NaOH PTSO to apatite formation on the surface can be show as follows. The Ti metal forms an apatite in the biological medium with NaOH. Metal is taken Na^+ ions from the surface. Through this ion exchange process, form sodium titanate. With the hydroxide ions coming from the 5 N NaOH PTSO, Ti-OH groups are formed. Ti-OH groups cause apatite nucleation, increasing the pH of the fluid support apatite formation with sodium ions (Kim *et al.* 2013, Faure *et al.* 2009). Karanjai *et al.* (2008) studied the TiO_2 phase on Ti-Ca-P composites by heat treatment. Increasing the TiO_2 phase in composite tend to increase apatite nucleation. In addition, bioactive phases are present in the composite. When the composite immersed in SBF, the following reaction have been taken place between TiO_2 and SBF;

$$TiO_2 + H_2O \leftrightarrow 2\ Ti\text{-}OH \quad (3)$$

Ti-OH groups have low free energy for nucleation of apatite, Na^+, HPO_4^{2-}, located in SBF is bonded the preferred sites, when the pH of the solution set to 7.4, and the ionic strength causes the pH to increase. Fan *et al.* (2009) in their study, HA60/316LSS biocomposites are immersed in SBF. Dissolving Ca^{2+} ions have been removed from the composite surface. Because of displacement of Ca^{2+} and H^+ ions, OH^- ions have been accumulated on the surface, in the end pH has been increased. It should be OH^- ions for apatite formation. According to the

mechanism of bone-like apatite formation, initially, biocomposite containing Ca^{2+} and P^{3-} ions have been immersed in SBF and then these ions on the surface dissolved and moved to SBF solution. Because of region of high concentration ions including apatite layer where a few crystal nuclei occurs, the super saturation of Ca^{2+} and P^{3-} ions is very low. The crystal nucleus adsorbs ions around them and develops their growth. Because adsorbed ions on biocomposite surfaces compete with each other. Fibrous and network-like Na-Ti-O compound responsible for nucleation and bone-like apatite occurs on the titanium substrate. This bone-like apatite layer implants can be an effective way to produce bioactive surfaces (Shi *et al.* 2001).

From the EIS plots (Fig. 3-4) it is clearly seen that, for the uncoated Ti-6Al-4V alloy, the phase angle drops to zero degree at very high frequencies, this showing that the impedance is controled by solution resistance in this frequency range. Furthermore, it should also be noted that the phase angle drops a bit towards little high characteristics in the low frequency area showing that the additive of polarization resistance to the impedance. The phase angle stays stability a wide frequency section supporting a near capacitive response for naked Ti-6Al-4V alloy. This situation is shown a characteristics fine passive oxide film on the surface of the uncoated alloy (Qui *et al.* 2010).

EIS plots (Fig. 3-4) are identified by two different sections: firstly in the more big frequency area owing to the reply of the electrolyte resistance and secondly in the formal and medium frequency area due to the answer of the capacitive attitude of the surface film. Existence of heterogeneities in the electrode-made tecnique should be due to terms of unusual conditions (Drevet *et al.* 2010).

3.2 SEM-EDX analyses results and discussions

SEM images of Ti6Al4V alloys are given Fig. 5 and EDX analysis is given Fig.6. The deposit at 85 ^{o}C (Fig. 5) was synthesized of agglomerates of species like platelets and big calcite crystals. Thermal expansion coefficient of HAP is higher than titanium, many fractures are composed of the HAP coating (Jiao and Wang 2009, Tian *et al.* 2010, Wei and Wang 2007) (Fig.5). When HAP coating is cooled selective temperatures, the thermal shrinkage mismatch results in the formation of cracks. Also, a significant sparking shrinkage during sintering results in the evolution of fractures in coatings as well (Wang *et al.* 2009). These fractures negative affect the bond of the layer on the surface. HAP formation does not correspond to the chemical reaction (Fig.6).

For this reason precipitating these ions indicates a Ca/P ratio less than 1.67, monetite ($CaHPO_4$) or brushite ($CaHPO_4.H_2O$) instead of HAP. The determined thickness and sticking of the HAP films with growing precipitation heat may be reported by three parts. Firstly, the solvabilities of both brushite and HAP reduce with rising temperature (Ding *et al.* 2003).

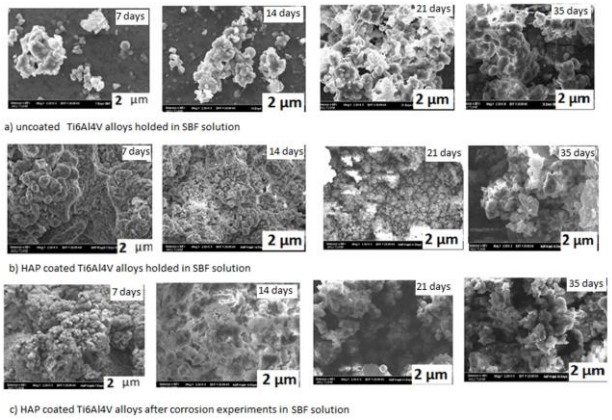

Figure 5. SEM images of Ti6Al4V alloys (different immersed times, uncoated, HAP coated and after corrosion experiments).

Thus the component of nucleation rate will increase, manufacturing Ca-P structure more probably to arise close to the Ti6Al4V.

Size deposition that requirements the hydroxide to scatter from the surface support film sediments. Secondly, a high increase deposition temperature give provides the deposition of a more fine film. If

the deposition temperature is more than 37 °C, fine crystalline film is obtained (Taş 2000). Thirdly, when the temperature is increase, on Ti6Al4V surface form less hydrogen gas, therefore little demolition is performed to the increasing Ca-P film. A fewer hydrogen bubbles is bond the surface and more of them is suspended in electrolyte (Fig. 6).

$$2H_2O + é \rightarrow H_2 \uparrow + 2OH^- \quad (4)$$

$$OH^- + H_2PO_4^- \rightarrow HPO_4^{2-} + H_2O \quad (5)$$

$$OH^- + HPO_4^{2-} \rightarrow PO_4^{3-} + H_2O \quad (6)$$

$$5Ca^{2+} + 3PO_4^{3-} + 2OH^- \rightarrow Ca_5(PO_4)_3(OH)_2 \quad (7)$$

The microstructure of this layer is uniform, and HAP forms needle-like shapes growing in a way vertical to the Ti6Al4V surface. Furthermore, the needle-like hydroxyapatite as a defined hexagonal crystal nature shows up. Moreover, when the unitial needle-like hydroxyapatite layer increasess to a particular degree, a large number of nucleation occurs over again at the high of the needle of HAP, and this circumstance can be seen at a higher SEM magnification.

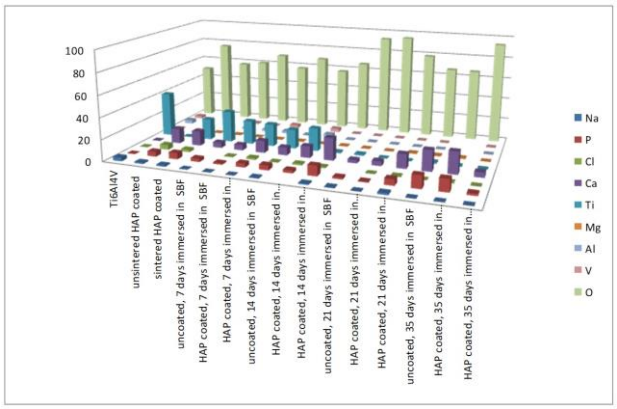

Figure 6. EDS analysis of Ti6Al4V alloys (different immersed times, uncoated, HAP coated and after corrosion experiments).

With the growth of a new nucleus, a new layer of small-grained HAP is formed. The amount of hydroxyapatite in the second layer increases as increased pretreatment time. When the Ti6Al4V substrate is dipped in the NaOH solution for a relatively little time, such as 12 h, almost only a small amount of sodium titanate gel appears on the substrate. As a consequence, only little Ti-OH groups are formed during hydrothermal electrochemical deposition. These a few Ti-OH groups encourage the evoluation of a HAP layer. Calcium phosphate coatings evaluated according to current density (Dumelie *et al.* 2005).

3.3 XRD analyses results and discussions

XRD spectrum of HAP coated unsintered is given Fig. 7 and HAP coated sintered Ti6Al4V alloy is given Fig. 8.

XRD results (Fig.7 and Fig.8) pointed out that hydroxyapatite is founded on the Ti6Al4V surface. Brushites, monetite, octacalcium phosphate, are known as precursors prior to HAP coating. Brushite more easily dissolves in SBF. In the HAP coating process on Ti6Al4V alloy surface contain two reactions the first is phosphate accumulation and growth, the second is hydrogen formation. Higher current densities increase hydrogen formation. This prevents the accumulation of phosphate (Djosic *et al.* 2012).

The difference between the thermal coefficients of HAP ($15{,}2x10^{-6}$ C^{-1}) and Ti6Al4V ($8{,}6x10^{-6}$ C^{-1}) cause micro cracks during cooling and heating the thickness of the HAP coating on Ti6Al4V substrate should not be less than 10 µm to avoid microcrack formation and mechanical degradation. Sintering should be 800 °C. TiO_2 film is excellent formed an interconnection between titanium substrate and HAP coating layer. After sintering, the addition of HAP pieces each other is occur more compact film. HAP coating behaved like an obstacle for the migration of electrons and ions (Nie *et al.* 2000). Between substrate and electrolyte HAP coating behave as barrier for move ions and electrons. Among substrate and electrolyte pores in HAP coating a conductive path occurs between the metallic conductor and the electrolyte ions HAP coating acts as a semi insulator layer to stop influence of the solution with the HAP coated substrate. Corrosion is occured with the diffusion of water and chloride ions into owing to the HAP coating. Electrochemical reactions continue between interface of HAP and Ti6Al4Vsubstrate.

The XRD results indicated that dicalcium phosphate dihydrate (DCPD), brushite ($CaHPO_4.2H_2O$) phasess were deposited. Rely on test stuations, the precipitation of unlike sorts of calcium phosphate coatings, e.g. dicalcium phosphate dihydrate (brushite, DCPD), hydroxyapatite (HA), octacalcium phosphate (OCP) and calcium-inadequate hydroxyapatite (Ca-def HAP) on the cathode is probable.

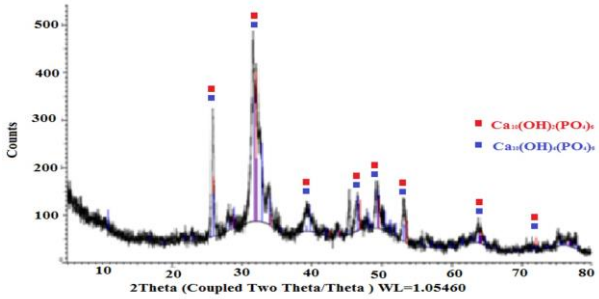

Figure 7. XRD spectrum of HAP coated unsintered Ti6Al4V alloy.

Four kinds of calcium phosphates in order of increasing solubility: $Ca_{10}(PO_4)_6(OH)_2$, $Ca_2(PO_4)_3{\cdot}nH_2O$, $Ca_8H_2(PO_4)_6{\cdot}5H_2O$, and $CaHPO_4{\cdot}2H_2O$ (Javidi *et al.* 2008). In the course of the deposition of calcium phosphates from aqueous solution, unlike calcium phosphates precipitation may be evaluated rely mainly on the pH worth of electrolyte.

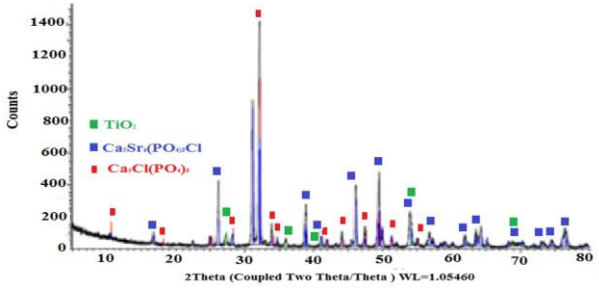

Figure 8. XRD spectrum of HAP coated sintered Ti6Al4V alloy.

As a result, the operation of electrochemical residue of coatings can be defined by electrochemical (hydrogen formation from distinct ions of the electrolyte and/or water molecules at elevated pH values as a side reaction), acid–base (consecutive pH-conditional passing between phosphates) and deposition reactions (deposition of Ca phosphates) (Ban and Hasegawa 2002, Rakngarm and Mutoh 2009, Javidi *et al.* 2008, Balamurugan *et al.* 2009, Kannan *et al*. 2005) When the pH value of the solution is same with the electrode surface, the calcium phosphate coating become visible. Unlike phosphates (e.g. $H_2PO_4^-$, $HPO4_2^-$ and PO_4^{3-}) are stable in dissimilar solutions and pH fields (Qui *et al.* 2010).

4. Conclusions

1. The uncoated TiAl4V alloy surfaces are observed to form like hydroxyapatite structures, after immersed in the SBF 7, 14, 21 and 35 days. Formations of HAP are increased as waiting time is rised.

2. The HAP coating has been successfully applied to NaOH surface pre-treatment electrodes by electrophoresis.

3. HAP coating has not been reduced the corrosion of Ti6Al4V alloy. The following factors have been effective in increasing the corrosion rate.

   a) During the electrochemical coating, a voltage of 4.5 V has been applied to the electrode with DC power supply.
   b) Sintering process has been made at high temperature (400-850^{o}C) in the muffle furnace after electrochemical coating.
   c) An inert atmosphere (such as argon in N_2) did not provide in the muffle furnace during sintering. Because there is not such system in the muffle furnace. For this reason, HAP coated specimens have been subjected to high temperature corrosion.

4. SEM, EDX and XRD analyzes show that various structure of HAP is formed on the surface.

Acknowledgements: The authors thanks to Afyon Kocatepe University BAP Coordination Unit for financial support (Project Number: 11.FENED.06).

5. References

Abdeltawab, A.A., Shoeib, M.A., Mohamed, S.G., 2011. Electrophoretic deposition of hydroxyapatite coatings on titanium from dimethylformamide suspensions. *Surface & Coatings Technology*, **206**, 43-50.

Balamurugan, A., Balossier, G., Michel, J., Ferreira, J.M.F., 2009. Electrochemical and structural evaluation of functionally graded bioglass-apatite composites electrophoretically deposited onto Ti6Al4V alloy. *Electrochimica Acta*, **54**, 1192-1198.

Ban, S., and Hasegawa, J., 2002. Morphological regulation and crystal growth of hydrothermal electrochemically deposited apatite. *Biomaterials*, **23**, 2965-2972.

Benea, L., Mardare-Danaila, E., Mardare, M., Celis, J.P., 2014. Preparation of titanium oxide and hydroxyapatite on Ti-6Al-4V alloy surface and electrochemical behaviour in bio-simulated fluid solution. *Corrosion Science*, **80,** 331–338.

Benea, L., Danaila, E., Ponthiaux, P., 2015. Effect of Titania anodic formation and hydroxyapatite electrodeposition on electrochemical behaviour of Ti-6Al-4V alloy under fretting conditions for biomedical applications. *Corrosion Science*, **91**, 262-271.

Bir, F., Khireddinea, H., Touati, A., Sidane, D., Yala, S., Oudadesse, H., 2012. Electrochemical depositions of fluorohydroxyapatite doped by Cu^{2+}, $Zn^{2+,}$ Ag^{+} on stainless steel substrates. *Applied Surface Science*, **258,** 7021-7030.

Blackwood, D.J. and Seah K.W.H., 2009. Electrochemical cathodic deposition of hydroxyapatite: Improvements in adhesion and crystallinity. *Materials Science and Engineering C*, **29,** 1233-1238.

Ding, S.J., Huang, T.H., Kao, C.T., 2003. Immersion behaviour of plasma-sprayed modified hydroxyapatite coatings after heat treatment. *Surface and Coatings Technology*, **165**, 248-257.

Djosic, M.S., Panic, M., Stojanovic, J., Mitric, M., Miskovic-Stankovic, M.V., 2012. The effect of applied current density on the surface morphology of deposited calcium phosphate coatings on titanium. *Colloids and Surfaces A: Physicochem. Eng. Aspects*, **400**, 36-43.

Drevet, R., Benhayoune, H., Wortham, L., Potiron, S., Douglade, J., Laurent-Maquin, D., 2010. Effects of pulsed current and H2O2 amount on the composition of electrodeposited calcium phosphate coatings. *Materials Characterization,* **61,** 786-795.

Du J., Liu X., He D., Liu P., Ma F., Li Q., Feng N., 2014. Influence of alkali treatment on Ti6Al4V alloy and the HA Coating deposited by hydrothermal-electrochemical methods. *Rare Metal Materials and Engineering,* **43(4),** 0830-0835.

Dumelie, N., Benhayoune, H., Rousse-Bertrand, C., Bouthors, S., Perchet, A., Wortham, L., Douglade, J., Laurent-Maquin, D., Balossier, G., 2005. Characterization of electrodeposited calcium phosphate coatings by complementary scanning electron microscopy and scanning-transmission electron microscopy associated to X-ray microanalysis. *Thin Solid Films*, **492**, 131-139.

Fan, X., Chen, J., Zou, J.P., Wan, Q., Zhou, Z.C., Ruan, J.M., 2009. Bone-like apatite formation on HA/316L stainless steel composite surface in simulated body fluid. *The Transactions of Nonferrous Metals Society of China*, **19**, 347-352.

Faure, J., Balamurugan, A., Benhayoune, H., Torres, P., Balossier, G., Ferreira, J.M.F., 2009. Morphological and chemical characterisation of biomimetic bone like apatite formation on alkali treated Ti6Al4V titanium alloy. *Materials Science and Engineering C*, **29**, 1252-1257.

Javidi, M., Javadpour, S., Bahrololoom, M.E., Ma, J., 2008. Electrophoretic deposition of natural hydroxyapatite on medical grade 316L stainless steel. *Materials Science and Engineering C*, **28**, 1509-1515.

Jiao, M.J. and Wang, X.X., 2009. Electrolytic deposition of magnesium-substituted hydroxyapatite crystals on titanium substrate. *Materials Letters*, **63**, 2286-2289.

Jonasova, L., Ullera, F.A.M., Helebrant, A., Strnad, J., Greil, P., 2004. Biomimetic apatite formation on chemically treated titanium. *Biomaterials*, **25**, 1187-1194.

Kannan, S., Balamurugan, A., Rajaeswari, S., 2005. Electrochemical characterization of hydroxyapatite coatings on HNO3 passivated 316L SS for implant application. *Electrochimica Acta*, **50**, 2065-2072.

Karanjai, M., Sundaresan, R., Raja, T., Mohan, R., Kashyap, B., 2008. Evaluation of growth of calcium phosphate ceramics on sintered Ti–Ca–P composites. *Materials Science and Engineering C,* **28**, 1401-1407.

Karthega, M., Raman, V., Rajendran, N., 2007. Influence of potential on the electrochemical behaviour of β titanium alloys in Hank's solution. *Acta Biomaterialia,* **3**, 1019-1023.

Kim, C., Kendall, M.R., Miller, M.A., Long, C.L., Larson, P.R., Humphrey, M.B., Madden, A.S., Tas, A.C., 2013. Comparison of titanium soaked in 5 M NaOH or 5 M KOH solutions. *Materials Science and Engineering C,* **33**, 327-339.

Kumar, M., Dasarathy, H., Riley, C., 1999. Electrodeposition of brushite coatings and their transformation to hydroxyapatite in aqueous solutions. *Journal of Biomedical Materials Research***, 45(4),** 302-310.

Kwok, C.T., Wong, P.K., Cheng, F.T., Manc, H.C., 2009. Characterization and corrosion behavior of hydroxyapatite coatings on Ti6Al4V fabricated by electrophoretic deposition. *Applied Surface Science*, **255**, 6736-6744.

Nie, X., Leyland, A., Matthews, A., 2000. Deposition of layered bioceramic hydroxyapatite/TiO_2 coatings on titanium alloys using a hybrid technique of micro-arc oxidation and electrophoresis. *Surface and Coating Technology*, **125**, 407-414.

Oh, S. and Jin, S., 2006. Titanium oxide nanotubes with controlled morphology for enhanced bone growth. *Materials Science and Engineering C,* **26**, 1301-1306.

Qiu, D., Wang, A., Yin, Y., 2010. Characterization and corrosion behavior of hydroxyapatite/zirconia composite coating on NiTi fabricated by electrochemical deposition. *Applied Surface Science,* **257**, 1774-1778.

Radice, S., Bradbury, C.R., Michler, J., Mischler, S., 2010. Critical particle concentration in electrophoretic deposition. *Journal of the European Ceramic Society,* **30,** 1079-1088.

Rakngarm, A. and Mutoh, Y., 2009. Electrochemical depositions of calcium phosphate film on commercial pure titanium and Ti–6Al–4V in two types of electrolyte at room temperature. *Materials Science and Engineering C*, **29**, 275-283.

Rath, P.C., Besra, L., Singh, B.P, Bhattacharjee, S., 2012. Titania/hydroxyapatite bi-layer coating on Ti metal by electrophoretic deposition: Characterization and corrosion studies. *Ceramics International,* **38**, 3209-3216.

Rigo, E.C.S., Boschi, A.O., Yoshimoto, M., Allegrini Jr., S., Konig Jr., B., Carbonari, M.J., 2004. Evaluation in vitro and in vivo of biomimetic, hydroxyapatite coated on titanium dental implants. *Materials Science and Engineering C,* **24**, 647-651.

Schmidt, H., Stechemesser, G., Witte, J., Soltanifarshi, M., 1998. Depth distributions and anodic polarization behaviour of ion implanted Ti6Al4V. *Corrosion Science,* 40, 1533-1545.

Shi J., Ding C., Wu Y., 2001. Biomimetic apatite layers on plasma-sprayed titanium coatings after surface modification. *Surface and Coatings Technology*, **137**, 97.

Song, Y.W., Shan, D.Y., Han, E.H., 2008. Electrodeposition of hydroxyapatite coating on AZ91D magnesium alloy for biomaterial application. *Materials Letters*, **62**, 3276-3279.

Stoch, A., Brożek, A., Kmita, G., Stoch, J., Rakowska, A., 2001. Electrophoretic coating of hydroxyapatite on titanium implants. *Journal of Molecular Structure,* 596, **1-3**, 191-200.

Taş, C., 2000. Combustion synthesis of calcium phosphate bioceramic powders. *Journal of the European Ceramic Society,* 20, 2389-2394.

Tian, A., Xue, X., Liu, C., He, J., Yang, Z., 2010. Electrodeposited hydroxyapatite coatings in static magnetic field. *Materials Letters,* 64, 1197-1199.

Wang, J., Chao, Y., Wan, Q., Zhu, Z., Yu, H., 2009. Fluoridated hydroxyapatite coatings on titanium obtained by electrochemical deposition. *Acta Biomaterialia*, **5**, 1798–1807.

Wei, Y. and Wang, X.X., 2007. Ribbon-like and rod-like hydroxyapatite crystals deposited on titanium surface with electrochemical method. *Materials Letters,* **61**, 4062-4065.

Zhang, Q., Leng, Y., Xin, R., 2005. A comparative study of electrochemical deposition and biomimetic deposition of calcium phosphate on porous titanium. *Biomaterials,* **26**, 2857-2865.